Chapter 5

Silver Diffusion Bonding and Layer Transfer of Lithium Niobate to Silicon

5.1 Introduction

In this chapter, we discuss a method of metallic bonding between two deposited silver layers. A diffusion bonding method has been developed that enables layer transfer of single crystal lithium niobate thin films onto silicon substrates. A silver film was deposited onto both the silicon and lithium niobate surfaces prior to bonding, and upon heating, a diffusion bond was formed. Transmission electron microscopy confirms the interface evolution via diffusion bonding which combines interfacial diffusion, power law creep and growth of (111) silver grains to replace the as-bonded interface by a single polycrystalline silver film. The layer transferred film, which was discussed in Chapters 3 and 5, had a composition that was the same as bulk lithium niobate. [1]

5.2 Wafer Bonding Limitations

Throughout the past two decades, wafer bonding has become an important electronics fabrication method [13, 114]. The ability to directly bond two materials, with varying lattice constants and crystal orientations, has facilitated the development of a wide range of research, from microelectromechanical systems to silicon-based photonics. Recently, wafer bonding processes have been combined with thin-film layer transfer induced by ion implantation. The combination of these two methods enables thin film single crystal layer transfer of a wide variety of semiconductors [14, 23, 48] and ferroelectrics [65, 87, 88]. By combining the flexibility of bottom-up processing with the near-ideal optical and electronic properties of single crystal films, these two techniques have become the standard method for producing silicon-on-insulator [23, 48]. In addition, wafer bonding and layer

[1] This chapter is based on work done with Dr. Melissa Archer and Dr. Jennifer Dionne [32].

transfer has enabled ultra-high efficiency, multi-junction solar cells to be fabricated by bonding lattice-mismatched semiconductors.

A major challenge with current layer transfer processes concerns the thermal mismatch and preparation of the two bonding surfaces. Direct bonding, with no adhesion layer, is always challenging, and depending on the materials, can prove to be nearly impossible. Previous work with lithium niobate and silicon showed difficulty in bonding due to the fact that the coefficient of thermal expansion mismatch between the two samples was too great. One technique that was examined to address this problem was using laser-induced forward transfer techniques [88]. This technique minimized thermal expansion mismatch between the two bonding layers by inducing layer transfer using a carbon dioxide laser rather than traditional thermal cycling. In addition to thermal considerations, extensive work is required to ensure surface planarity, smoothness, and cleanliness of the two surfaces [9, 123, 129]; however, such processes are expensive and inefficient. Further, many of the methods used to produce bondable surfaces can ruin the implantation process and prevent a layer from being transferred. This problem could be circumvented with a reliable method for bonding two roughened or otherwise non-ideal surfaces.

The use of a metallic bond has been extensively developed for use in the 3D integrated circuit industry using copper and gold interconnects. Extensive research on copper bonding has been reported in dozens of publications by the group of Professor Reif at MIT as well as a wide range of other research departments [25, 26]. Besides gold and copper, another metal in the same category of materials is silver. Throughout this thesis and the literature, silver is used extensively in plasmonics research for its exceptional loss characteristics in regards to waveguides, resonators, and modulators [21, 35, 36, 109]. The development of a silver-silver diffusion bond which would allow single crystal active layers to be bonded to virtually any type of substrate significantly increases the flexibility of designing novel plasmonic structures. This design could also be extended towards the design of multi-layered MIM or other waveguiding structures which, without a robust and flexible metal bonding layer, might otherwise not be possible.

The rest of this chapter will focus on developing this new type of silver-silver bond which is used to improve the lithium niobate to silicon bond that was discussed in Chapter 4. Further, this type of bond is not limited to the two materials discussed here; rather, this technique allows single crystal thin films of a wide variety of materials to be transferred onto virtually any type of substrate. Finally, the experimental measurements done here indicate that the bonding mechanism which enables the silver-silver diffusion bond is similar to that seen in gold and copper.

5.3 Experimental Work

Polished, x-cut lithium niobate single crystal samples were obtained from MTI Corporation. Following the work done in Chapter 3, these samples were co-implanted with hydrogen to 6×10^{16} ions/cm^2 at 80 keV, followed by a 115 keV helium implantation with a dose of 5×10^{16} ions/cm^2. All implantations were done at room temperature. The lithium niobate and silicon (100) substrates were then sequentially sonicated in methanol, acetone, isopropanol, and deionized water. Silver was concurrently evaporated on both the implanted lithium niobate and silicon substrates (without removal of the silicon native oxide layer) to a thickness of 400 nm at 2.5 $\mathring{A}/s$. The roughness of the deposited silver was measured using atomic force microscopy, and the contamination of the silver surfaces before bonding was measured using X-ray photoelectron spectroscopy. The silvered surfaces were then bonded together at $500°C$ for four hours in a nitrogen environment. The high temperature anneal caused the silver layers to bond together. Simultaneously, the anneal induced crack formation within the lithium niobate layer, following the formalism developed in Chapter 4, at the peak implantation depth. As a result, a layer of lithium niobate, whose thickness corresponds to the peak depth of ion implantation and whose area corresponded to the entire 1 cm^2 sample, was transferred to the silicon handle substrate.

Using a focused ion beam, transmission electron microscopy samples were extracted from both the bonded lithium niobate/silver/silicon sample and a silicon (100) substrate with 400 nm of silver evaporated on it under the same conditions as the bonded sample. Before milling, a 1 μm thick platinum layer was locally deposited on the sample to prevent ion-induced lattice damage. The bonded structure was milled into on both sides of the TEM lamella and a U-shaped pattern was cut into the silicon to ease in the removal process, Figure 5.1(a). Using the focused ion beam, micro-tweezers were milled into a disposable tip within the FIB and the width of the micro-tweezers was milled such that they were the same size as the thicker portion of the lamella. The tweezers were then slid onto the thick portion of the lamella, Figure 5.1(b). After the lamella was secured with tweezers, the remaining portions of the U-cut were removed with the FIB and the lamella was able to be removed with the tweezers, Figure 5.1(c). After extraction, the thinner portion of the lamella was thinned from the size with deposited platinum to the point where the thin region of the lamella was 50 nm thick. This was done using gallium ions with an accelerating voltage of 30 keV. The samples were then characterized using a transmission electron microscope, which was operated at 300 keV.

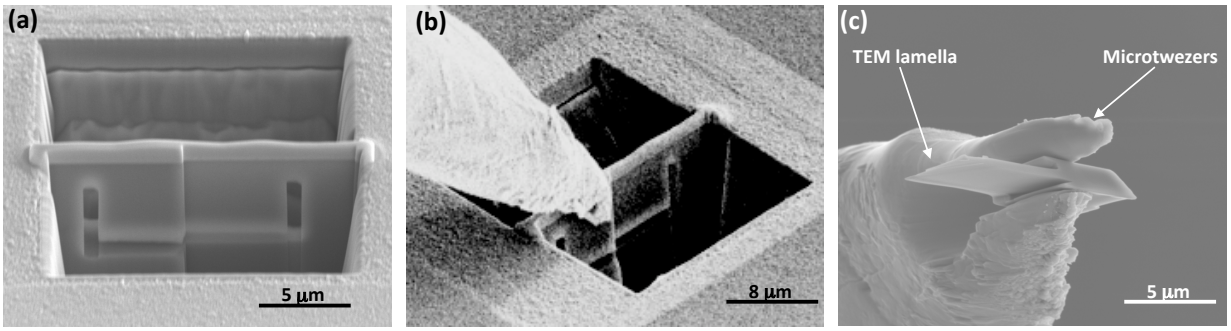

Figure 5.1. Removal of a sample for TEM using the FIB. (a) shows the initial milled structure before it's removed from the substrate. The lamella is then held using the micro-tweezers (b) and the rest of the lamella is released from the substrate. Finally, the FIB thins down the thinner portion of the lamella to 50 nm in preparation for TEM.

5.4 Analysis of Silver Diffusion Bonding

Figure 5.2(a) shows the lithium niobate sample with the silicon substrate at the bottom, the silver layer as the dark central region, the lithium niobate above it, and the 1 μm thick platinum layer in the top right section of the image. The silver layer, which appears as a dark band through the middle of the sample, appears to be continuous from one interface to the other and shows no sign of the original interface between the two silver layers. The lithium niobate layer is shown in detail in Figure 5.2(b). From this image, strain contrast from the bonding process can be seen at the interface between the transferred layer and the silver layer (bottom left). This can be attributed to the mismatch in the coefficients of thermal expansion between the silicon, silver, and x-cut lithium niobate layers (2.6×10^{-6}, 19.1×10^{-6}, and 8.2×10^{-6} K^{-1} respectively [58]). Through the center of the transferred film, a defect free single crystal region exists. This is seen in the selected area diffraction pattern shown as an inset, in which the crystal orientation corresponds with the x-cut orientation of the original lithium niobate sample. Above the single crystal region, a region of lattice damage remains as a result of the ion implantation and platinum deposition processes. To address this issue, we refer back to Chapter 3 which showed that a secondary annealing step, after the bonding step, can significantly remove any residual lattice damage from the layer transfer process and return the transferred layer to its original, single crystal state [87].

X-ray photoelectron spectroscopy confirmed the existence of a thin oxide layer on the surface of the deposited silver films before bonding and atomic force microscopy determined that the root-mean-squared roughness of that surface was $\sim$ 7.0 nm. Unlike gold which will start to form a

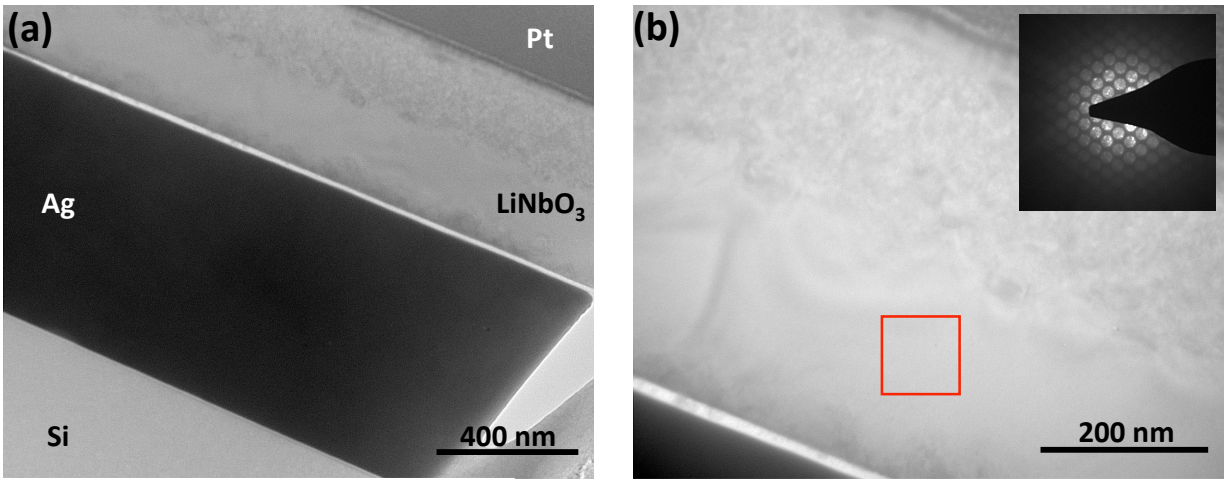

Figure 5.2. Transmission electron image of the extracted lamella, (a). From bottom to top the layers are: silicon, the bonded silver layer, lithium niobate, and the protective platinum layer. At higher magnification, the lithium niobate layer, (b), shows a strained interface, followed by a single crystalline region, and finally an amorphous damage region left over from the ion implantation. The diffraction pattern (inset) was taken in the region enclosed by the red box.

diffusion bond under pressure at room temperature, the silver oxide layer was sufficient to prevent bonding from occurring at room temperature. The samples were initially brought together at room temperature, such that the two silver films only contacted at the asperities of each silver surface. Upon heating to $500°C$, the silver oxide layer became thermodynamically unstable [76, 77], and diffusion bonding took place. This process, which has been previously investigated for other materials systems by Derby and Wallach [29, 30, 47], consisted of an initial, rapid process of plastic deformation of the asperities of both silver films. Such deformation results in formation of a series of elliptical voids at the fractionally bonded interface. These voids are clearly visible in both scanning electron microscope and transmission electron microscope images, as shown in Figures 5.3(a) and (b) respectively.

After the initial stage of plastic deformation, the interfacial voids are removed during the remainder of the bonding process. Voids are removed through a combination of surface diffusion at the void/silver interface, bulk diffusion and grain growth, and power law creep [29, 30, 47]. All three mechanisms contribute to the removal of the bonding interface simultaneously, and the degree to which each mechanism contributes is determined by the bonding material, time, temperature, pressure, and initial surface conditions.

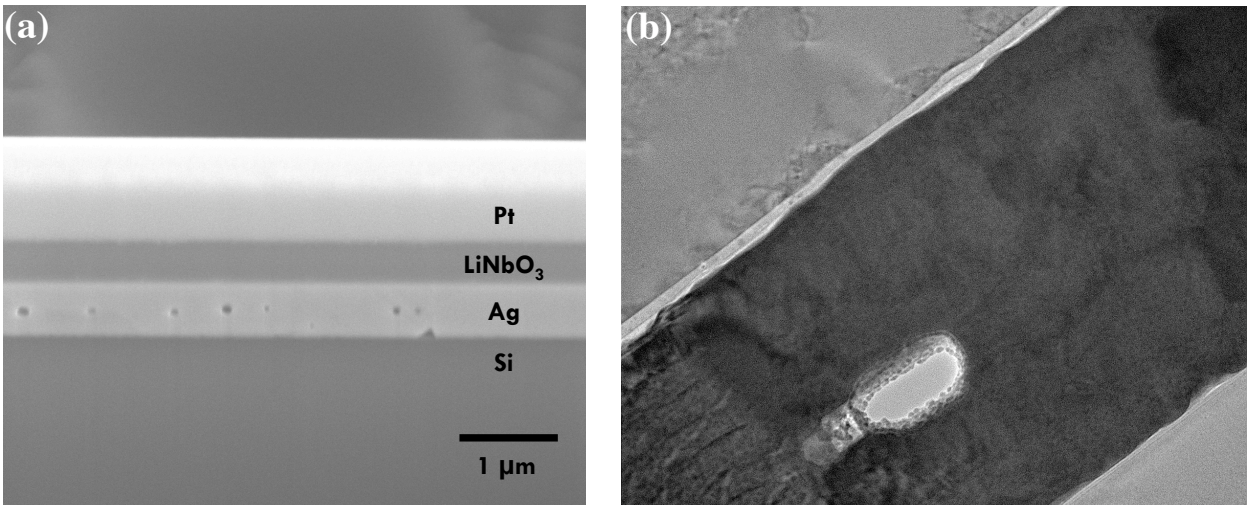

Figure 5.3. Scanning electron microscope image of the lithium niobate bonded to silicon with a silver bonding layer, (a). Ellipsoidal voids can be seen half way through the partially bonded silver layer. A transmission electron microscope image of one of the voids, (b), shows an intermediate stage between initial contact of the two silver layers and complete bonding, Figure 5.4(d).

During the bonding process, significant grain growth occurs through the bonding interface, as well as in the plane of the silver film. As opposed to imaging silver films with the SEM, when using the FIB to image silver, there is significant channeling of Ga^+ ions at the silver grain boundaries. As a result, imaging these surfaces with the focused ion beam produces a very clear image of the individual grains within a silver film. These images, before and after annealing, show that the average as-deposited grain size was 53 nm, whereas after the annealing the average grain size was 400 nm, as shown in Figures 5.4(a) and (b) respectively. X-ray diffraction analysis of identical samples of the silver films before and after the annealing process show that the grain growth observed is a result of preferential growth of silver (111) grains during the annealing process, Figure 5.5. Transmission electron microscope images of the silver layer before and after bonding are shown in Figures 5.4(c) and (d). The sample prior to bonding in Figure 5.4(c) exhibits multiple grains whose diameters are small enough that they do not extend throughout the thickness of the film. In contrast, grains extend across the original silver-silver interface after bonding, as shown in Figure 5.4(d). Three grains within the silver film extending from the silicon interface to the lithium niobate interface are shown. Note that the in-plane grain size in Figure 5.4(d) is also significantly larger than in 3(c). As in Figure 5.2(b), the interface between the two un-bonded silver layers is completely removed after bonding. Also, within each grain the film is single crystalline from the

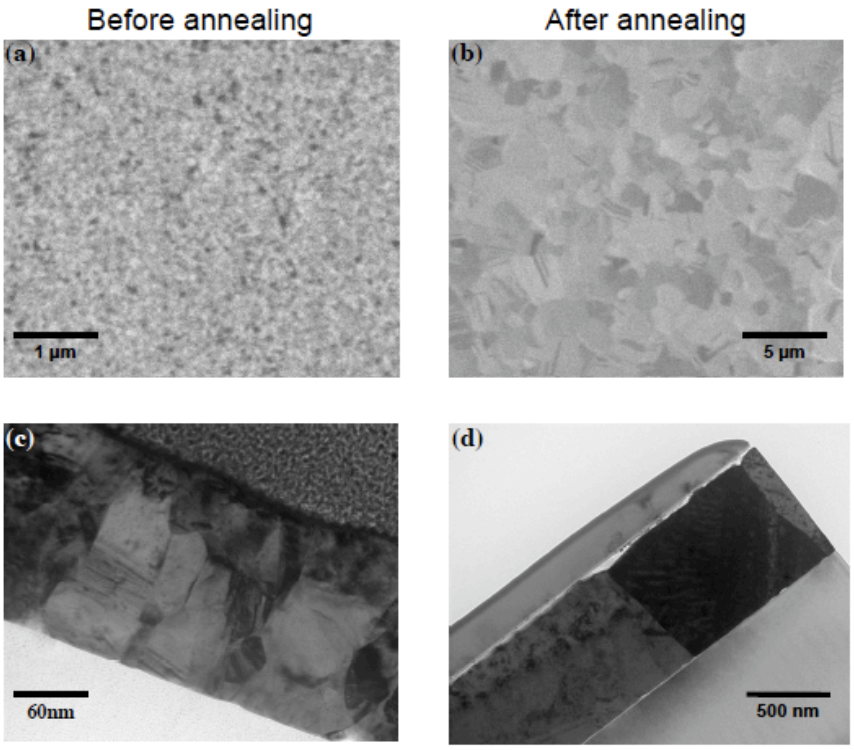

Figure 5.4. Focused ion beam images of the deposited silver films before and after annealing, (a) and (b) respectively. The average grain sizes were 53 nm in (a) and 400 nm in (b). Transmission electron microscope images of the silver layer before and after bonding, (c) and (d) respectively, show that grain growth during the annealing process has completely removed the interface between the original silver bonding layers.

silicon interface to the lithium niobate interface.

After the initial bonding process is complete, if further high temperature processing steps are required, the diffusion bonding process would continue based on the new time, temperature, and pressure conditions. Assuming the initial heating cycle produces a void-free bond, bonding would occur through a combination of bulk diffusion and grain growth, along with power law creep. This would further increase the size of the grains that extend from the silicon/silver interface to the lithium niobate/silver interface.

Finally, we note that the use of this method could generate deep level traps within the silicon substrate [50]. With a diffusivity on the order of 10^{15} cm^2/s in silicon [78], certain device applications that are dependent on minority carrier lifetimes could be affected. For those devices where silver concentration within the silicon is a concern, a thin diffusion barrier could be deposited

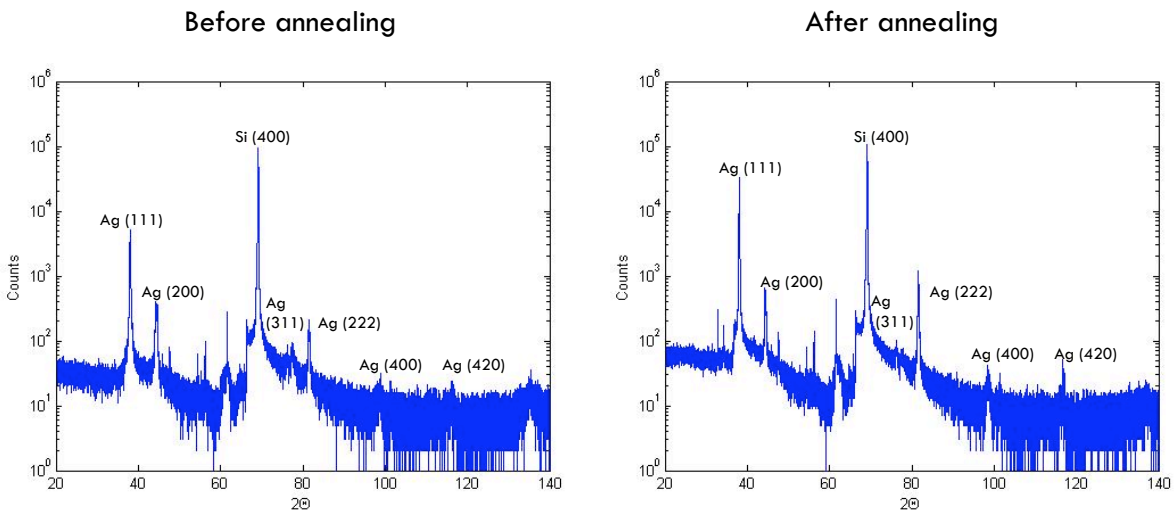

Figure 5.5. X-ray diffraction measurements of silver films before and after the annealing process associated with layer transfer. The growth of Ag (111) grains is one of the main mechanism is the formation of the silver bond.

between the silver and silicon [19]. Provided the processing temperature of such a device is kept below $500 - 600°C$, these layers could be used to prevent adverse silver diffusion.

5.5 Conclusion

In this chapter we developed a new method of metallic bonding using two deposited silver layers. In combination with ion implantation-induced layer transfer, this technique has been demonstrated as a method for layer transfer of single crystal lithium niobate onto silicon substrates. This process, which can also be done with gold and copper, allows a wide variety of single crystal active layers to be bonded to virtually any type of substrate, and this technique increases the flexibility of designing novel plasmonic structures. We've shown that bonding between the two deposited silver layers occurred as a result of diffusion bonding which is similar to the processes that have been examined with gold and copper. Scanning electron microscopy and transmission electron microscopy images show that this process completely removed the bonding interface, and within individual grains, the silver was single crystalline from the lithium niobate/silver interface to the silicon/silver interface.

The combination of proper ion implantation (Chapter 3), with a proper choice of coefficient of thermal expansion matched materials (Chapter 4), and an improved bond strength using silver-silver diffusion bonding (Chapter 5), allows us to fabricate MIM waveguides with silver as the

cladding layers and lithium niobate as the active material. The results of this work are discussed in the following chapter.